Culturing of the first 37:4 predominant lacustrine haptophyte: geochemical, biochemical, and genetic implications

Jaime L. Toney[1], Susanna Theroux[1,2], Robert A. Andersen[3], Annette Coleman[4], Linda Amaral-Zettler[1,2], Yongsong Huang[1]

[1]Department of Geological Sciences, *Brown University*

[2]The Josephine Bay Paul Center for Comparative Molecular Biology and Evolution, Marine Biological Laboratory

[3]Provasoli-Guillard National Center for Culture of Marine Phytoplankton

[4]Molecular Biology, Cell Biology & Biochemistry, *Brown University*

ABSTRACT

Long chain alkenones (LCAs) are potential biomarkers for quantitative paleotemperature reconstructions from lacustrine environments. However, progress in this area has been severely hindered by the lack of culture studies of haptophytes responsible for alkenone distributions in lake sediments: the predominance of $C_{37:4}$ LCA. Here we report the first enrichment culturing of a novel haptophyte phylotype (Hap-A) from Lake George, ND that produces predominantly $C_{37:4}$-LCA. Hap-A was enriched from its resting phase collected from deep sediments rather than from water column samples. In contrast, enrichments from near surface water yielded a different haptophyte phylotype (Hap-B), closely related to *Chrysotila lamellosa* and *Pseudoisochrysis paradoxa*, which does not display $C_{37:4}$-LCA predominance (similar enrichments have been reported previously). The LCA profile in sediments resembles that of Hap-A enrichments, suggesting that Hap-A is the dominant alkenone producer of the sedimentary LCAs. In enrichments, excess lighting appeared to be crucial for triggering blooms of Hap-A. Both U^K_{37} and U^K_{38} indices show a linear relationship with temperature for Hap-A in enrichments, but the relationship appears to be dependent on the growth stage. Based on 18S rRNA gene analyses, several lakes from the Northern Great Plains, as well as Pyramid Lake, NV and Tso Ur, Tibetan Plateau, China contain the same two haptophyte phylotypes. The Great Plains lakes

35 show the Hap-A-type LCA distribution, whereas Pyramid and Tso Ur show
36 the Hap-B type distribution. Waters of the Great Plain lakes are dominated
37 by sulfate, whereas those Pyramid and Tso Ur are dominated by carbonate,
38 suggesting that the sulfate to carbonate ratio may be a determining factor for
39 the competitiveness of the Hap-A and Hap-B phylotypes in natural settings.
40

1. INTRODUCTION

Sedimentary long-chain alkenones (LCAs) produced by haptophyte algae have been widely and successfully used for sea surface temperature reconstructions for decades (Brassell et al., 1986; Prahl and Wakeham, 1987). Recent studies revealed that LCAs are also very common in lakes, especially saline lakes, worldwide (Cranwell, 1985; Zink et al., 2001; Chu et al., 2005; D'Andrea and Huang, 2005; Pearson et al., 2008; Toney et al., 2010; Theroux et al., 2010). However, the use of lacustrine LCAs as a paleotemperature proxy is less straightforward than for ocean systems because different species of haptophytes may reside in different lakes and may require different temperature calibrations (Coolen et al., 2004; D'Andrea and Huang, 2005; Theroux et al., 2010). Extensive sampling of the water column at different depths and seasons from the study lakes offers one viable solution to the calibration problem (Toney et al., 2010). However, the ultimate solution to understanding the response of lacustrine haptophyte algae to environmental parameters (e.g., temperature) is to culture the organism in question, as has been extensively carried out for ocean haptophytes, *Emiliania huxleyi* and *Gephyrocapsa oceanica* (e.g., Volkman et al., 1980; Volkman et al., 1995).

One distinctive feature of LCA distributions in lake sediments is the exceptionally high abundance of tetra-unsaturated C_{37} alkenone ($C_{37:4}$) in many lakes (Cranwell, 1985; Volkman et al, 1988; Thiel et al., 1997; Wang

63 and Zheng, 1998; Zink et al., 2001; Sun et al., 2007; Chu et al., 2005;
64 D'Andrea and Huang, 2005; Toney et al., 2010). However, to date, no
65 laboratory has been able to capture and culture the lacustrine alkenone-
66 synthesizers that produce such LCA signature profiles. Reported enrichments
67 from lakes have found species closely related to *Chrysotila lamellosa* (e.g, Sun
68 et al., 2007), which do not produce predominantly $C_{37:4}$ LCA (Sun et al., 2007,
69 Rontani et al., 2004). A recent environmental molecular survey of lake
70 surface sediments (Theroux et al., 2010) further highlights the problem:
71 multiple species of haptophyte algae are present in lakes worldwide and
72 *Chrysotila lamellosa* represents only one type of haptophyte. Many lakes
73 show overlapping distributions of species, which are not necessarily defined
74 by biogeography. Although different haptophyte DNA phylotypes do not
75 necessarily denote different temperature sensitivities, the results point to a
76 major gap in our understanding of lacustrine haptophyte species. The
77 mismatch between the cultured lacustrine haptophytes and the sedimentary
78 LCA signatures, and the lack of cultures for lake species that produce the
79 $C_{37:4}$-dominant profile, represent major barriers to the application of alkenone
80 proxy for paleotemperature reconstructions in lake sediments.
81
82 We present in this paper the first successful enrichment of a lacustrine
83 haptophyte, referred to as Hap-A, that produces predominantly $C_{37:4}$
84 alkenone from Lake George, ND. We used unusual conditions to maintain

this organism, which may account for previous unsuccessful attempts to establish cultures. In addition to Hap-A, we also maintain enrichments of Hap-B that are closely related to *Chrysotila lamellosa*. We used 18S rRNA gene analyses to determine the phylogenetic placement of our Lake George haptophyte species and Fluorescence *In Situ* Hybridization (FISH) experiments to visualize haptophytes in our enrichments. We discuss the implications of these findings with respect to modern LCA production and application to paleotemperature reconstructions.

2. METHODS

2.1. Field and sampling methods

Water and sediment samples were collected from Lake George, North Dakota (46.74°N, 99.49°W) in June of 2009 with a Van Dorn water sampler and an Ekman grab sampler. Two 1-liter water samples were collected at 5-m, 6-m and 10-m depths, while sediment samples were collected from the near-shore, oxic environment at 5-m depth and from the deep basin of the lake at 44-m depth (See Table 1). One 1-L water sample from each depth was filtered using a vacuum filtration unit with combusted (550°C) GF/F 0.7μm, 47 mm glass filters. Additional water was collected in June of 2010 for the second set of experiments. Twelve liters were collected from the surface water and filtered with a 0.2μm Micropore (Pall Corporation, Michigan) filter to use as stock water and 1-L was collected at 5-m depth, unfiltered.

2.2. Enrichment Methods

2.2.1. Experiment 1: producing LCAs in enrichments

Six enrichments (A, B, C, D, E, and F) were started on June 9, 2009 in 2-L Erlenmeyer culture flasks in a growth chamber at 20°C during light and 18°C during dark, 68% humidity, and a 12-hr:12-hr, light:dark cycle using different initial starting materials (details in Table 1). These growth chamber conditions were maintained until February 15, 2010. After this date, light intensity was increased so that the surface of the enrichment water received 200μmol m^{-2} s^{-1} (previous light settings were ~100μmol m^{-2} s^{-1}). Enrichments A, B, and D were started from 1-L unfiltered lake water with added f/2 nutrient medium (NaH_2PO_4 – 1ml/1-L, vitamin – 0.5ml/1-L, trace metal – 1ml/1-L, $NaNO_3$ 1ml/1-L; to prevent diatom blooms Si was not added) (MKF220L-CCMP) (Guillard, 1975), while enrichment C and E were started from 30-cc of sediment in 1-L of lake water filtered at 0.7μm and inoculated into f/2 nutrient medium. For enrichment F, 50-ml of unfiltered lake water was added to seawater from Boothbay Harbor, Maine that was brought down to Lake George salinity 9.7 g L^{-3} with distilled water and inoculated with f/2 nutrient medium. 15-ml subsamples were collected from the enrichments on June 24, July 15, August 15, and November 15 of 2009 and on April 18, 2010. Growth chamber temperature was increased to 25°C on April 19, 2010 and enrichments were subsampled again on May 2, 2010.

129

130 *2.2.2. Experiment 2: testing temperature dependence of LCAs in enrichments*

131 To test the effect of growth temperature (4°C, 10°C, and 20°C) on the
132 alkenone unsaturation index, twelve liters (12 L) of Lake George water were
133 filtered through a 0.2μm Millipore (Pall Corporation, Michigan) filter into an
134 autoclaved storage container. One hundred milliliters was sent to the
135 Colorado Plateau Stable Isotope Laboratory for analysis of major anion and
136 cation water chemistry. Three control enrichments were set up in 2-L
137 Erlenmeyer flasks that contained 1-L filtered (0.2 μm) lake water plus f/2
138 medium. Three, unfiltered water and three, deep-sediment enrichments were
139 set up by adding 50-ml of unfiltered lake water or 30-cc of deep sediment to 1
140 L of 0.2 μm-filtered Lake George water and f/2 medium. Culture flasks were
141 placed in three separate growth chambers (4°C, 10°C, and 20°C with 12hr
142 light:dark cycle, light intensity of at the top of the enrichment water surface
143 was 200μmol m^{-2} s^{-1}) so that each chamber had a control, unfiltered, and deep
144 sediment treatment. Enrichments were started on June 28, 2010. Every ~15-
145 days (July 13, July 27, August 10, August 25) a 10-ml subsample of water
146 was collected in a 15-ml centrifuge tube to test for alkenones with care taken
147 not to disturb any sediment at the bottom of the culture flask. On August 25,
148 samples of the agitated water and sediment were collected to analyze both
149 the living and sedimentary organics. Centrifuge tubes were stored in a
150 freezer, freeze-dried and then run for organic analysis (see Section 2.4).

151

152

153 **2.3. 18S rRNA Gene Analyses**

154 *2.3.1. DNA extraction*

155 Subsamples were collected for DNA analyses from enrichments A-F in April,
156 2010. Fifteen milliliters of sample were filtered onto a 0.2μm Sterivex
157 (Millipore, Billerica, MA) filter, flooded with lysis buffer (Qiagen, City, State),
158 and kept frozen at -20°C until processing. Samples were extracted using the
159 Gentra Puregene Tissue Kit (Qiagen, Valencia, CA 158667) according to the
160 manufacturer's instructions. Total extracted genomic DNA was quantified
161 using a NanoDrop nucleic acid spectrophotometer (Thermo Scientific,
162 Wilmington, DE).

163

164 *2.3.2. DNA amplification and sequencing*

165 Genomic DNA was amplified using haptophyte specific primers (Simon et al.,
166 2000; Coolen et al., 2004) targeting 18S rRNA coding regions. Forward and
167 reverse primers correspond to *Escherichia coli* 16S rRNA positions 429 and
168 887, respectively. Polymerase chain reactions (PCRs) were performed on an
169 Eppendorf Gradient Thermocycler (Eppendorf, Hamburg, Germany) with the
170 following conditions after D'Andrea et al., (2006): 4 min initial denaturing at
171 96 °C, 35 cycles of denaturing for 30 s at 94 °C, followed by 40 s primer
172 annealing at 55 °C and primer extension 40 s at 72 °C, with a final extension

of 10 min at 72 °C. PCR products were purified using the Purelink PCR purification kit (Invitrogen, Carlsbad, CA). Cloning was performed using the Invitrogen TOP10 cloning kit with electro- competent cells. The protocol followed the manufacturer's instructions. Ten clones were picked for each sample. Plasmid DNA was isolated using a RevPrep Orbit robotic template preparation instrument (Genomic Solutions, Ann Arbor, MI), and prepared templates were sequenced on an ABI 3730XL (Applied Biosystems, Foster City, CA) capillary sequencer using the BigDye protocol with universal M13 forward and reverse primers according to the manufacturer's instructions. All sequencing was performed at the Marine Biological Laboratory W. M. Keck Ecological and Evolutionary Genetics Facility.

2.3.3. Bioinformatics and phylogenetic reconstructions

A bioinformatics pipeline using the programs phred, cross-match, and phrap, translated chromatograms into base-calls and associated quality scores, removed vector sequences and assembled forward and reverse reads into full-length sequences for each of the cloned PCR amplicons (Ewing and Green, 1998; Ewing et al., 1998). Only sequences greater than 400 bp and with a complete forward and reverse primer were retained. Base-calls were verified and sequences were manually edited with the program Consed (Gordon et al., 1998) for chromatogram viewing. Assembled sequences were aligned using the ARB software program v. 07.07.11 (Ludwig et al., 2004) against the

October 2008 Silva 96 Ref database (Pruesse et al., 2007) using the FastAligner option followed by manual adjustment. Sequences were aligned with reference haptophyte sequences and subjected to a Bayesian analysis after Theroux et al., (2010).

2.3.4. Fluorescence *In Situ* Hybridization

Subsamples (5-ml) were collected from each enrichment during week 4 of the temperature experiments. Cells were probed using a haptophyte-specific oligonucleotide probe PRYM02 (Simon et al., 2000) modified with an Alexa488 fluorophore (Invitrogen, City, State). Cells were concentrated via centrifugation and preserved in 80% ethanol for three days at -20°C to remove as much autofluorescence as possible. Cells were vortexed in hybridization buffer (18µl 5M NaCl, 2 µl 1M Tris-HCL pH 7.4, 1 µl 1% SDS, 20µl 100% formamide, 1 µl Probe (0.2 nmol/µl), 58 µl distilled H_2O) and incubated at 46°C for 2-hours. Cells were centrifuged and resuspended in wash buffer (4.3µl 5M NaCl, 2µl 1M Tris, 1µl 1% SDS, 92.7µl distilled H_2O) and incubated at 48°C for 15 min. Cells were centrifuged and resuspended in wash buffer, mounted onto an agar coated slide, and dried at room temperature for 1-hr. Slide was mounted with Citiflor:Vectashield (4:1 v/v) (London) to preserve probe fluorescence. Slides were viewed and photographed on a Zeiss Axioskop 2 MOT.

2.4. Lipid analysis

Freeze-dried water and sediment samples were homogenized and extracted with dichloromethane (DCM):methanol (MeOH) (9:1, v/v) using an Accelerated Solvent Extractor ASE200 (Dionex). Fifty microliters of C_{36} *n*-alkane standard (72.43 μg ml^{-1}) were added, and the total lipid extracts (TLEs) were run on a GC-FID for detection and quantification of alkenones using the internal standard. An Agilent DB-1 GC column (60 m × 320 μm × 0.10 mm) was used with the following temperature program: an initial temperature of 40°C (hold 1-min), ramp 30°C min^{-1} to 290°C (hold 1-min), ramp 5°C min^{-1} to 300°C (hold 0-min) then 2°C min^{-1} to 325°C, GC temperature program (hold 10-min) (Toney et al., 2010). The same temperature program was used on the GC-MS, and samples were run to confirm the identity of the alkenones using the known ion chromatograms and by comparison of mass spectral data with published data and GC retention times (de Leeuw et al., 1980, Marlowe et al., 1984). The final GC program described here is the result of testing many permutations of GC parameters, including the switch from helium as the carrier gas to hydrogen. As such we are able to resolve LCAs with >4μg per sample (i.e. grams of dry sediment or liter of water). Alkenone standards of known temperature calibration were run on the GC-MS to ensure analytical precision (<0.1°C).

3. RESULTS

239 **3.1. Long-chain alkenone distribution and temperature dependence**

240 *3.1.1. Experiment 1: confirming LCA production in enrichments*

241 Of the six enrichments (A, B, C, D, E, and F), none produced LCAs based on
242 organic analysis of the 15-ml subsamples collected on June 24, July 15,
243 August 15, and November 15 of 2009 (Table 1). However, LCAs were present
244 in relatively high concentrations (ranging from 10.4 to 1191 μg L^{-1}) in all
245 enrichments, except enrichment F, in subsamples that were collected on April
246 18, 2010. Notably, the alkenone distributions for enrichments A-D were very
247 similar with $C_{37:3}$ dominance (76±2%) over other C_{37} LCAs and $C_{38:3}$ both
248 ethyl and methyl forms dominant over other C_{38} LCAs. Whereas, in
249 enrichment E, $C_{37:4}$ was dominant (54%) and $C_{38:3}$, the ethyl homologue,
250 dominated the C_{38} LCAs (Figure 1; Table 1). The temperature was inferred
251 from the LCA unsaturation index (U_{37}^{K}) calibration using a linear regression
252 model ($T = 48.4982 \times U_{37}^{K} + 42.1494$) that was specifically developed using an
253 *in situ* relationship derived for the LCAs of Lake George (Toney et al., 2010).
254 Using this relationship, inferred temperatures from the U_{37}^{K} for enrichments
255 A-D produce temperatures much higher (38±1.6°C) than the diurnal growth
256 temperature range of 18°C to 20°C. Inferred temperature from enrichment E
257 produces a temperature of 18.9°C, which is within the range of the diurnal
258 temperature cycle of the growth chamber. None of the enrichments produced
259 LCAs following the increase in temperature to 25°C.

260

3.1.2. Experiment 2: testing temperature dependence of LCAs in enrichments

New experiments were designed to determine if production of LCAs could be replicated using the same enrichment techniques as above and to test the temperature dependence of the LCAs. The control treatment at 20°C produced no LCAs throughout the sampling period, however, the controls at 4°C and 10°C both produced LCAs with distributions similar to enrichments A-D on July 13, July 27 and August 10 (Table 3). On August 25, only the control at 4°C contained LCAs. Flasks that were started with unfiltered lake water collected at 5-m depth (herein unfiltered enrichments) also did not produce LCAs at 20°C, while the 4°C unfiltered enrichment produced LCAs in similar distributions as enrichments A-D on July 27, and the 10°C unfiltered enrichment produced similar LCAs on July 27 and August 10 with barely detectable amounts on August 25. The enrichment started from the deep sediment (herein deep enrichments) produced LCAs on all collection days with distributions similar to enrichment E at all temperatures until August 25, when only the 10°C enrichment produced LCAs. On August 25, agitated water/sediment samples were collected from the deep enrichment. Only deep enrichments at 4°C and 10°C contained LCAs. The major anion and cation concentrations of the enrichment water are presented in Table 2.

3.2. 18S rRNA gene analyses

From enrichments A-E, the control, unfiltered, deep-sediment enrichments and isolated subsamples of enrichment C (246, 478, 481, 484), we identified two Operational Taxonomic Units (OTUs). Each enrichment had only one of the two OTUs. The OTU associated with enrichments started from the water column and shallow sediments is referred to as Hap-B, whereas the OTU associated with enrichments started from deep sediments are referred to as Hap-A.

We constructed a phylogenic tree using a representative sequence from each OTU with previously published haptophyte 18S rRNA genes (Figure 2). The tree topology is similar to that published by Theroux et al., (2010) with the new Lake George, ND OTUs branching with OTU7 and OTU8, which were previously reported from the surface sediments of Lake George and other U.S. and Chinese lakes.

4. DISCUSSION

In this paper we present the results of two separate enrichment experiments. The first experiment consisted of starting enrichments from different parts of the lake system (e.g. water column, sediment) in an attempt to produce LCAs under controlled conditions (Section 4.1.). The second experiment used the information gained from the initial enrichments to test the temperature

dependency of LCAs (Section 4.2.). We combined these techniques with 18S rRNA gene sequencing (Section 4.3.) to confirm the identity of the haptophyte species present in the enrichments. We also used FISH (Section 4.4.) to visualize haptophytes in the enrichments.

4.1. Long-chain alkenone production in enrichments

4.1.1. The role of water chemistry on LCA production in enrichments

Our enrichment data show that water chemistry strongly affects the production of LCAs. LCAs were present in relatively high concentrations in enrichments A-E that were grown in native Lake George water. However, LCAs were not produced in enrichment F, which was initiated by adding 50 mL of Lake George water to f/2 medium prepared with a seawater base that was adjusted to Lake George salinity. The base water is the only variable in the culture medium used to establish enrichments A and F, which suggests the lake water chemistry is important for LCA production. The major ion chemistry is significantly different for seawater and Lake George (Table 2). The cation chemistry is similar for the seawater and Lake George. Both are dominated by Na^+, but in seawater it is ~28-times more abundant than Mg^{2+}, Ca^{2+}, and K^+. For Lake George, Na^+ is 8-times more than Mg^{2+}, 12-times more than K^+, and 260-times more than Ca^{2+}. The anion chemistry is completely different, with the dominant anion in seawater, Cl^-, and the dominant anion in Lake George, SO_4^{2-}. We diluted the seawater so that the salinity was

326 equivalent (Mg^{2+} and Na^{+}), thus it is the anion chemistry that may control
327 the presence and production of LCAs, although Ca^{2+} may also be important.
328 The anion chemistry supports previous findings from the Northern Great
329 Plains, where the absolute concentration of major anions did not appear to
330 affect the LCA distribution, but the $C_{37:4}$-producing haptophytes were only
331 found in lakes with sulfate-to-carbonate ratios (SCR) greater than one (Toney
332 et al., 2010). Here the diluted seawater has a SCR of 0.14, whereas, the Lake
333 George water SCR is 21 (Table 2).
334
335 *4.1.2. Light as an important trigger LCA production in Hap-A enrichments*
336 Enrichments did not produce LCAs until nearly a year following their start
337 date with light intensity held constantly at ~100 μmol m^{-2} s^{-1}. The field water
338 used to start these enrichments was collected at end of bloom season and
339 suggests that we captured the resting phase of the haptophyte that does not
340 produce LCAs. Although nutrients and trace metals were ample in the
341 enrichments beginning in June of 2009, the haptophytes were not triggered
342 into an active, LCA-producing phase until sometime between November 2009
343 and April of 2010. The only changes that occurred in this window of time
344 were the passing of time and the intensification of light. It is possible that the
345 resting phase of the haptophytes is time sensitive and that overwintering
346 occurs for a certain length of time each year. However, our enrichment
347 methods did revive haptophytes from the deep sediments, regardless of the

348 time of year in subsequent experiments (see Section 4.2.), which suggests
349 time is not likely the trigger. Alternatively, the intensification of light from
350 ~100 μmol m^{-2} s^{-1} to 200 μmol m^{-2} s^{-1} in February of 2010, may have triggered
351 the haptophytes into an active stage that produces LCAs. This supports the
352 hypothesis by Toney et al., (2010) that increased light penetration following
353 ice-off in the spring causes the haptophytes to rise from the bottom of Lake
354 George and produce LCAs during the haptophyte bloom.
355
356 *4.1.3. Enrichment starting materials on LCA distributions*
357 Based on lipid signatures and 18S rRNA gene sequencing, we enriched for
358 what appear to be two distinct phylotypes of haptophyte algae, Hap-A and
359 Hap-B. Among the five, LCA-producing enrichments, enrichments A through
360 D (Hap-B) produce LCAs with the same distribution, while enrichment E
361 (Hap-A) produces LCAs with a different distribution (Figure 1). 18S rRNA
362 gene analysis confirms that the haptophyte present in enrichment E (Hap-A)
363 is genetically distinct from the haptophyte present in enrichments A-D (Hap-
364 B) (See Section 4.3. and Figure 2). The DNA sequencing results from each
365 enrichment yielded only one haptophyte phylotype each, and suggest that
366 Hap-A and Hap-B do not coexist in the enrichments. The distribution of LCAs
367 in enrichment E is most similar to the sedimentary alkenone profile (Figure
368 1) and the water column LCAs during *in situ* sampling of the 2008 and 2009
369 spring blooms (Toney et al., 2010). The concentration of LCAs produced by

haptophytes in enrichments A through D ranged from ~10 to 150 μg L^{-1}, while the concentration of LCAs was an order of magnitude higher in enrichment E (~1200 μg L^{-1})(Table 1). The similar profiles of LCA distributions suggests that the LCAs produced by Hap-A are the dominant contributor to the sedimentary LCAs, which may be due primarily to the vast production rates or competitive exclusion of Hap-B. However, it is also possible that predation may also be important in delivering alkenones to the sediment via fecal pellets. Not enough is known about the community ecology during the bloom or the form of delivery to sediments to speculate further at this time.

The organism producing the Hap-A phylotype and the predominant $C_{37:4}$ LCA distribution, appears to have different initial enrichment condition requirements than Hap-B. These differences suggest a possible different ecological strategy for the two haptophytes within the lake. The Hap-A phylotype is found in the deep surface sediments (~47 m), while Hap-B appears to be enriched from various parts of the lake water column and shallow sediments. It is possible that Hap-A needs a substrate in its resting phase, but if this were the only requirement, then we should also find Hap-A in the enrichments started from the shallow sediments. Instead, the deep sediments may provide refuge from predation over the winter for Hap-A.

These enrichment data provide new insights into the previous *in situ* sampling and temperature calibration from Lake George. Two statistical outliers occur in the Toney et al., (2010) calibration. Upon reanalysis, these outliers' chromatograms resemble the distributions from Hap-B with the presence of the C_{38}:3 methyl ketone. These data points were collected in the water column at the surface and at 5 m, when we hypothesize the bloom of Hap-A had already moved down to 10-m depth. This suggests that Hap-B is adapted to thrive following the Hap-A bloom when lower nutrient conditions prevail. These Hap-B characteristic LCAs were present only in very low concentrations (< 27 μg L^{-1}) and resulted in inferred-temperatures that were too high for the Hap-A-based calibration. As a result, this led us to believe that lacustrine environments are subject to similar issues as marine environments, where low concentrations of alkenones produce high inferred-temperature, which is often attributed to instrumental bias when concentrations of LCAs are at or below the detection limit (see Rosell-Melé et al., 1995 and Rosell-Melé et al., 2001). At Lake George, however, low concentrations and high-inferred temperatures are the result of a different LCA-producing haptophyte species.

The requirement of different starting materials and enrichment conditions suggest that the sedimentary resting phase, potential cyst production, is important for phylotype Hap-A's adaptive strategy. Although little is known

about the benthic stages of haptophytes or the factors that affect the transition between different stages (Boalch 1987; Rousseau et al., 1994), our enrichment results suggest that Hap-A and Hap-B have two very different survival strategies. Based on the information that we have at present, Hap-A rests at the bottom of the lake until conditions (e.g., light, nutrients, etc.) are favorable, blooms, and then settles back to the resting phase when nutrients become scarce. Hap-B, alternatively, is adapted to survive under lower nutrient conditions after the onset of thermal stratification and increased competition with diatoms, green algae, and cyanobacteria following Hap-A's bloom. Previous studies have shown that Lake George is N-limited at this time in the seasonal lake cycle (Salm et al., 2010) and suggests that under N-limiting conditions, Hap-B would be more abundant than Hap-A.

4.1.4. Relationship of LCA distribution and indices to enrichment conditions

Two distinct groups of haptophytes have previously been identified based on their LCA distribution in the Northern Great Plains lakes (Toney et al., 2010) and their DNA sequences from surface sediments (Theroux et al., 2010). Carbonate-dominated lakes in Nebraska produced LCA distributions that lacked $C_{37:4}$, while northern, sulfate-dominated lakes produced LCAs dominated by $C_{37:4}$. It is unclear how similar the C_{37}:$_3$-producing Hap-B phylotype is to the haptophyte(s) in the Nebraska sites that appear to lack $C_{37:4}$ because attempts to amplify DNA from the sediments of Nebraska lake

436 sites during analyses by Theroux et al., (2010) were unsuccessful. The
437 Nebraska lake LCA profiles are likely produced by a different haptophyte and
438 suggests that there maybe at least three different haptophyte species in the
439 lakes of the Great Plains. Theroux et al., (2010) did find that two different
440 haptophyte phylotypes amplified from Lake George surface sediments. These
441 data are compared with the enrichment DNA sequences detailed below in
442 Section 4.3. Despite the existence of two haptophyte species in Lake George,
443 it appears that the sedimentary profile is dominated by the Hap-A profile in
444 the modern environment (Figure 1). It is possible, however, that at times in
445 the past lake environmental conditions favored Hap-B and it is important to
446 know how their presence may affect LCAs as a paleotemperature proxy.
447
448 The ratio of C_{37}:C_{38} LCAs has been used to distinguish different haptophyte
449 species in other studies (e.g., Pearson et al., 2009). There is a large difference
450 between the C_{37}:C_{38} ratio of LCAs from the Nebraska (2.4) versus Northern
451 Great Plains (4.6) lake sites (Toney et al., 2010), however, there is only a
452 subtle difference between the C_{37}:C_{38} ratio between Hap-B (1.3±0.1) and Hap-
453 A (1.8). The overall ratios from the enrichments are lower than the samples
454 collected in the field, however, which suggests that there are secondary
455 controls on this ratio (i.e. nutrients, dissolved oxygen, salinity). U^{K}_{37}, $U^{K'}_{37}$ and
456 U^{K}_{38} indices describe the degree of unsaturation in the LCA distribution. These
457 indices have been related to growth temperature in previous studies,

458 although only $U^{K'}_{37}$ was temperature sensitive in the *in situ* work from Lake
459 George (Toney et al., 2010). These indices were calculated for LCAs in all the
460 enrichments (Table 1). The $U^{K'}_{37}$ and U^{K}_{38} indices for Hap-B are not significantly
461 different from Hap-A, however, the U^{K}_{37} index is significantly different (-
462 0.08±0.03 versus -0.48). Using the linear regression model (T = 48.4982 ×
463 U^{K}_{37}+ 42.1494) specifically developed for the LCAs of Lake George on the
464 unsaturation indices calculated from Hap-B produces temperatures much
465 higher (38±1.6°C) than the diurnal growth temperature range of 18°C to
466 20°C. Inferred temperature from Hap-A produces a temperature of 18.9°C,
467 which is within the range of the diurnal temperature cycle of the growth
468 chamber. This lends support to the observation that the Hap-A phylotypte is
469 the major contributor to the sedimentary LCAs, and is also the haptophyte
470 responsible for LCA production during the spring bloom from which the
471 calibration was derived.
472
473 **4.2. Experiment 2: Replicating enrichment methods and LCA**
474 **temperature dependence**
475 New experiments were designed to show that production of LCAs could be
476 replicated using similar culturing techniques as above and to test the
477 temperature dependence of the enrichment-produced LCAs. A control that
478 contained only Lake George 0.2 μm-filtered water was not expected to contain
479 LCAs throughout the experiment, however, at 4°C and 10°C the controls

480 produced LCAs with distributions similar to Hap-B enrichment (Table 3).
481 One possibility is that because LCAs are 62Å in size, they could have passed
482 through in the filtering process, however, none were detected at 20°C and the
483 concentration of LCAs in the 4°C and 10°C controls increased with time.
484 These results suggest that active production of LCAs occurred in the controls.
485 Similarly, the enrichments started from unfiltered lake water produced Hap-
486 B-type distributions at 4°C and 10°C.
487
488 Based on our E enrichment, we hypothesize that Hap-A and Hap-B
489 phylotypes compete with each other during temperature experiments. The
490 enrichments started from the deep sediment produced Hap-A LCAs at all
491 temperatures until week 8, when only the 10°C enrichment produced a trace
492 amount (34μg L^{-1}) of LCAs that resembled the Hap-B LCA profile. The
493 agitated water/sediment samples were collected from the deep enrichment in
494 week 8 when relatively high concentrations (>600μg L^{-1}) of LCAs were found
495 in the 4°C and 10°C enrichments. These distributions were dominated by
496 $C_{37:4}$ at 4°C and by $C_{37:3}$ at 10°C. The 4°C enrichment produced an inferred
497 temperature of 4.9°C using the *in situ* water column calibration, while the
498 10°C enrichment produce a temperature of 25°C with the *in situ* calibration
499 and 11.9°C with the known *C. lamellosa* calibration (Sun et al., 2007).
500 Notably, the 10°C deep enrichment's agitated, lipid profile showed clear
501 methyl- and ethyl-$C_{38:3}$ peaks and indicates that under the enrichment

conditions, the Hap-B phylotype out-competed the Hap-A phylotype at 10°C. The enrichments were not set up under chemostat conditions, meaning that the nutrients were allowed to decline throughout the experiment. This is likely why Hap-B was able to out-compete Hap-A as time progressed. As the bloom period progressed in all sediment enrichments, the percentage of $C_{37:4}$ decreased (Figure 3), suggesting that the Hap-B phylotype became active once the Hap-A phylotype began to decline. This suggests that Hap-B is adapted to conditions with decreased nutrients and potentially warmer temperatures that prevail toward the end of the bloom as observed in the environmental, *in situ* calibration (see Section 4.1.3.).

Only the Hap-A enrichment U^{K}_{37} and U^{K}_{38} indices were temperature dependent during the experiments (Figure 3). The unfiltered and control enrichments did not produce LCAs at 20°C, so a calibration is not possible and there are no significant differences in U^{K}_{37}, $U^{K'}_{37}$ or U^{K}_{38} at different temperatures. For the Hap-A enrichment, $U^{K'}_{37}$ shows no temperature dependency, but U^{K}_{37} and U^{K}_{38} indices show a linear relationship with temperature in week 6 and week 2 respectively (r^2 = 0.998 and 0.950)(Figure 3). These two indices have nearly the same relationship to temperature, but are offset from the *in situ* calibration. The relationship is offset to higher unsaturation values and may indicate different relationships between LCAs and temperature at different growth stages. Alternatively, the offset could be due to a larger contribution

524 from the Hap-B phylotype that produces less $C_{37:4}$ relative to $C_{37:3}$ and is
525 favored under these enrichment conditions, but not in the environment
526 during *in situ* calibration sampling. The presence of Hap-B phylotype is
527 evident in the LCA profile that shows a decreasing percentage of $C_{37:4}$ and an
528 increased presence of $C_{38:3me}$. The similarity in slopes, despite the different
529 phylotype producer has been found in other studies (D'Andrea and Bradley,
530 2010) and suggests that while a universal, absolute temperature calibration
531 is not possible for lakes, the slope ($dU_{37}^{K}/d\ temperature$) may be used to derive
532 the change in temperature through time. From the enrichments and Lake
533 George *in situ* samples a 0.013 change in U_{37}^{K} occurs per 1°C, although the
534 range in U_{37}^{K} is relatively high, 0.017 for *in situ* samples and 0.011 for
535 enrichments. At Lake George, careful inspection of the $C_{38:3}$ LCAs for the
536 presence of methyl homologues is the most appropriate way to determine if
537 the calibration can be applied to a particular sample. The presence of methyl
538 homologues indicates that temperatures may be influenced by Hap-B LCAs
539 and appear artificially high.
540
541 **4.3. Phylogenetic relationships with previously reported**
542 **haptophytes**
543 Our phylogenetic analyses indicated that distinctions observed between the
544 two different lipid profiles are attributable to two different haptophyte
545 phylotypes (Figure 2). Hap-B from the shallow lake environment branches

546 with two known haptophyte taxa (*Chrysotila lamellosa*, *Pseudoisochrysis*
547 *paradoxa*) and one unidentified sequence from Greenland's Lake HundeSø
548 (Theroux et al., 2010). In particular, the Hap-B sequence is identical in the
549 region sequenced for the OTU7 representative sequence that was previously
550 reported from Lake George, Medicine Lake, Skoal Lake, Great Salt Lake,
551 Pyramid Lake, Keluke Hu, and Tso Ur[1]. The lipid profiles for *C. lamellosa*
552 and for surface sediments from the Great Salt Lake, Pyramid Lake, and Tso
553 Ur are similar to those from the enrichments from which the Hap-B
554 phylotype DNA sequences were amplified and have $C_{37:4}$ present, but not
555 dominant. The Hap-B lipid profile differs from *C. lamellosa*, however, because
556 it produces both $C_{38:3et}$ and $C_{38:3me}$ homologues, whereas *C. lamellosa* only
557 produces $C_{38:3et}$ (Rontani et al., 2004). The lipid distribution for surface
558 sediments from Lake HundeSø, Lake George, Medicine Lake, and Skoal Lake
559 are all dominated by $C_{37:4}$, which suggests that although OTU7 is present,
560 LCA production in these lakes is dominated by a different haptophyte
561 species. The masking of the OTU7-type lipid profile in the sedimentary
562 record suggests that, like Lake George, this producer does not produce high
563 concentrations of alkenones.
564
565 Based on the placement of the Hap-A phylotype on the phylogenetic tree and
566 comparison of sequences, this species is likely closely related to the OTU8

[1] Note: Tso Ur is located in the central Tibetan Plateau (31.48, 91.52) and has multiple names including: Cuo E, Tibetan Plateau Central Lake B, and Co Ngoin.

567 representative sequence that has been reported from Lake George, Medicine
568 Lake, Skoal Lake, Pyramid Lake, Keluke Hu, Tso Ur and Clear Lake. The
569 surface sediments from Lake George, Medicine Lake, and Skoal Lake have
570 lipid profiles similar to Hap-A enrichments, whereas Pyramid and Tso Ur
571 have lipid profiles similar to Hap-B. These differences in lipid profiles suggest
572 that in the first set of lakes (LG, ML, SL), the lipid profile associated with
573 OTU8 phylotype dominates; whereas in the latter set of lakes (PY, TU) the
574 OTU7 phylotype dominates the lipid production. Despite extensive field
575 sampling, we have not found that the OTU7-phylotype lipid profile dominates
576 in any part of the Lake George natural system spatially or temporally.
577 Therefore, it is worth examining the differences between these two sets of
578 lakes to determine if there are conditions that favor one species over the
579 other, aside from the short-term, low nutrient advantage for the Hap-B
580 phylotype as discussed above in Section 4.1.3.
581
582 Lake water chemistry plays a major role in determining whether Hap-A or
583 Hap-B phylotype is the dominant producer in lakes where both are present.
584 Physical parameters, geochemistry, and salinity of lakes with OTU8 (LG,
585 ML, SL) have previously been reported (Toney et al., 2010). Similar
586 parameters have also been reported for Pyramid Lake (Galat et al., 1983) and
587 Tso Ur (Wu et al., 2009), where the OTU7 phylotype dominates the lipid
588 production. The physical lake parameters (depth, volume, etc.) vary among

589 all the lakes, and salinity ranges from 5 to 12 g L^{-1} with no significant
590 differences between the two sets of lakes (Table 4). The major cation in all
591 lakes is Na^{+}. The main difference between the two sets of lakes is the major
592 anion chemistry. Lakes where the OTU8 phylotype dominates the lipid
593 production are dominated by SO_4^{-2}, whereas, HCO_3^{-} and CO_3^{-2} dominates in
594 Pyramid Lake and Tso Ur (Wu et al., 2009). The sulfate to carbonate ratio
595 (SCR) for the first set of lakes is much greater than one (between 32 and
596 117), while the SCR for Pyramid Lake and Tso Ur is less than one (0.24 and
597 0.40, respectively). This supports the importance of SO_4^{-2} for the production of
598 LCAs dominated by $C_{37:4}$. Based on previous studies, the lowest SCR value for
599 LCAs dominated by $C_{37:4}$ is 8.2; whereas, the highest value for Hap-B
600 distributions is 2.6 (Toney et al., 2010). This suggests that the *in situ*
601 temperature calibration derived for Lake George should work in mid-latitude,
602 evaporative lakes with OTU8, where SCR is > 8.2. Below SCR of 1, we would
603 expect that the OTU8 phylotype to be outcompeted by the OTU7 phylotype, if
604 present. The exact threshold for the dominance of OTU8 (Hap-A) versus
605 OTU7 (Hap-B) is not determined here, and would require further
606 investigations and manipulation of Hap-A and Hap-B enrichments. We have
607 not yet developed a U_{37}^{K} calibration for the Hap-B phylotype, but further
608 investigations in lakes where the OTU7/Hap-B phylotype dominates the lipid
609 production would reveal more information about this species, which does not
610 appear to compete as well in our high sulfate lakes. The conclusion from

these two sets of lakes suggests that our outlying, down-core samples from Lake George reflect brief transitions to a lake system dominated by HCO_3^- and CO_3^{-2} anions or are severely nutrient depleted.

4.4. Size differences between Hap-A and Hap-B from FISH analyses

From the FISH analyses, we were able to visualize two different algae that fluoresced with the PRYM02 haptophyte primer. The first was a small (<10 μm) cell (Figure 4) from enrichments A-D, control and unfiltered enrichments from the temperature experiment, and likely represents Hap-B phylotype cells. The second, from the sediment derived enrichments was ~20μm (Figure 4), and likely represents Hap-A phylotype cells.

5. CONCLUSION

The laboratory enrichment of two distinct haptophyte phylotypes from Lake George, ND provides new insights into conditions necessary to grow the predominant-$C_{37:4}$ producing lacustrine haptophyte. The enrichments also provide suggestions about the competing environmental controls on the two haptophytes found and their biosynthesis of LCAs. Specifically, we showed that: (1) Lake George haptophytes can survive a wide range of geochemical conditions, but produced LCAs in enrichments only when sulfate is dominant over carbonate; (2) haptophytes began to produce LCAs under enrichment

conditions after being triggered by increased light intensity; (3) the haptophyte responsible for the production of the lipid profile dominated by $C_{37:4}$ (Hap-A) was only found by 'reviving' the algae from its resting phase in the deep sediments rather than water column samples; whereas, the haptophyte that produces the *C. lamellosa*-like lipid profile (Hap-B) was only found in enrichments from the water column and shallow sediments; (4) the Hap-A phylotype produces LCAs in concentrations an order of magnitude higher than the Hap-B phylotype; (5) the Hap-A phylotype dominates the sedimentary signature and is the species from which the *in situ* calibration was developed; (6) the Hap-B phylotype is distinguishable by the presence of $C_{38:3me}$; (7) Hap-B may have an adaptive advantage under low nutrient conditions; (8) U^K_{37} and U^K_{38} indices show a linear relationship with temperature, but the relationship appears to be dependent on the growth stage or offset due to interference by Hap-B; (9) the main difference leading to the dominance of the Hap-A signature over the Hap-B signature appears to be the anion geochemistry, mainly Hap-A prefers sulfate.

Despite the enrichment-based findings and evidence for competition between Hap-A and Hap-B phylotypes, the core-top, sedimentary LCAs record the temperature of the surface water bloom for Hap-A. This suggests that as a community, Hap-A LCA production occurs in the surface waters before migrating back down to the sediments for overwintering. Also, the

655 sedimentary LCAs can be used to infer temperature if caution is used to
656 detect and discard samples with $C_{38:3me}$ LCAs, indicative of Hap-B phylotype
657 alkenone production. Future analyses of Lake George haptophyte
658 enrichments may reveal additional environmental and physiological
659 intricacies of alkenone production by these novel taxa.
660
661 *Acknowledgements*: This work was supported by a grant from the National
662 Science Foundation to Y. Huang (EAR06-02325) and a Brown University
663 Graduate School Dissertation Fellowship to J. L. Toney.
664

665 **REFERENCES**

666 Boalch, G.T. (1997) Recent blooms in the Western English Channel. *Rapport*
667 *du P.V. Réunion Conseil International pour l'Exploration de la Mer* 187:94-97
668
669 Brassell S.C., Eglinton G., Marlowe I.T., and Sarnthein M. (1986) Molecular
670 stratigraphy: a new tool for climatic assessment. *Nature* **320**, 129-133.
671
672 Chu G., Sun Q., Li S., Zheng M., Jia X., Lu C., Liu J., and Liu T. (2005) Long-
673 chain alkenone distributions and temperature dependence in lacustrine
674 surface sediments from China. *Geochimica et Cosmochimica Acta* **69**, 4985-
675 5003.
676
677 Coolen M.H., Muyzer G., Rijpstra W.I.C., Schouten S., Volkman J.K., Damsté
678 J.S.S. (2004) Combined DNA and lipid analyses of sediments reveal changes
679 in Holocene haptophyte and diatom populations in an Antarctic lake. *Earth*
680 *Planet. Sci. Lett.* **223**, 225-239.
681
682 Cranwell P.A. (1985) Long-chain unsaturated ketones in recent lacustrine
683 sediments. *Geochimica et Cosmochimica Acta* **49**, 1545-1551.
684

685 D'Andrea W.J. and Huang Y. (2005) Long-chain alkenones in Greenland lake
686 sediments: Low $\delta^{13}C$ values and exceptional abundance, *Organic*
687 *Geochemistry* **36**, 1234-1241.
688
689 D'Andrea, W.J. and Bradley, R.S. (2010) A 5,000 year alkenone-based
690 temerature record from Lower Murray reveals a distinct Medieval Warm
691 Period in the Canadian High Arctic, *EOS* 2010AGUFM43C-10D.
692
693 de Leeuw J.W., van der Meer F.W., and Rijpstra W.I.C. (1980) On the
694 occurrence and structural identification of long chain unsaturated ketones
695 and hydrocarbons in sediments. In *Advances in Organic Geochemistry 1979*
696 (ed. A.D. Douglas and J.R. Maxwell), pp. 2311-2317. Pergamon.
697
698 Ewing, B. and Green, P. (1998) Base-calling of automated sequencer traces
699 using phred. II. Error probabilities. *Genome Res.* **8,** 186-194.
700
701 Ewing, B., Hillier, L., Wendl, M.C., Green, P. (1998) Base-calling of
702 automated sequencer traces using phred. I. Accuracy assessment. *Genome*
703 *Res.* **8**, 175-185.
704

705 Galat, D.L. and Robinson, R. (1983) Predicted effects of increasing salinity on
706 the crustacean zooplankton community of Pyramid Lake, Nevada.
707 *Hydrobiologia* **105**, 115-131.
708
709 Gordon, D., Abajian, C., Green, P. (1998) Consed: a graphical tool for
710 sequence finishing. *Genome Res*. **8**, 195-202.
711
712 Guillard R.R.L. (1975) Culture of phytoplankton for feeding marine
713 invertebrates. in "*Culture of Marine Invertebrate Animals*." (eds: Smith W.L.
714 and Chanley M.H.) Plenum Press, New York, USA. pp 26-60.
715
716 Ludwig, W., Strunk, O., Westram, R., Richter, L., Meier, H., Yadhukumar,
717 Buchner, A., Lai, T., Steppi, S., Jobb, G., forster, W., Brettske, I., Gerber, S.,
718 Ginhart, A.W., Gross, O., Grumann, S., Hermann, S., Jost, r., Konig, A., LIss,
719 T., Lussmann, R., May, M., Nonhoff, B., Reichel, B., Strehlow, R., Samatakis,
720 A., Stckmann, N., Vilbig, A., Lenke, M., Luwig, T., Bode, A., Schleifer, K.H.
721 (2004) ARB: a software environment for sequence data. *Nucleic Acids Res*. **32**,
722 1363-1371.
723
724 Marlowe I.T., Brassell S.C., Eglinton G., and Green J.C. (1984) Long chain
725 unsaturated ketones and esters in living algae and marine sediments.
726 *Organic Geochemistry* **34**, 261-289.

727

728 Pearson E.J., Juggins S., and Farrimond P. (2008) Distribution and
729 significance of long-chain alkenones as salinity and temperature indicators
730 in Spanish saline lake sediments. *Geochimica et Cosmochimica Acta* **72**,
731 4035-4046.

732

733 Prahl F.G. and Wakeham S.G. (1987) Calibration of unsaturation patterns in
734 long-chain ketone compositions for palaeotemperature assessment. *Nature*
735 **330**, 367-369.

736

737 Pruesse, E., Quast, C., Knittel, K., Fuchs, B.M., Ludwig, W.G., Peplies, J.,
738 glockner, F.O. (2007) SILVA: a comprehensive online resource for quality
739 checked and aligned ribosomal RNA sequence data compatible with ARB.
740 *Nucleic Acids Res*. **35**, 7188-7196.

741

742 Rontani, J., Beker, B., Volkman, J.K. (2004) Long-chain alkenones and
743 related compounds in the benthic haptophyte *Chrysotila lamellosa* Anand
744 HAP17. *Phytochemistry* **65**, 117-126.

745

746 Rosell-Melé, A., Carter, J.F., Parry, A.T., Eglington, G. (1995) Determination
747 of the UK37 Index in geological samples. *Anal. Chem*. **67**, 1283-1289.

748

749 Rosell-Melé, A., Bard, E., Emeis, K.C., Grimault, J.O., Müller, P., Schneider,
750 R., Bouloubassi, L., Epstein, B., Fahl, K., Fluegge, A., Freeman, K., Goñi, M.,
751 Güntner, U., et al., (2001) Precision of the current methods to measure the
752 alkenone proxy Uk'37 and absolute alkenone abundance in sediments:
753 Results of an interlaboratory comparison study. *Geochmistry, Geophysics,*
754 *Geosystems* **2**, 1046.
755
756 Rousseau, V., Vaulot, D., Casotti, R., Cariou, V., Lenz, J., Gunkel, J.
757 Baumann, M. (1994) The life cycle of *Phaeocystis* (Prymnesiophyceae):
758 evidence and hypotheses. In: *Ecology of Phaeocystis-dominated Ecosystems*
759 (Ed. by C. Lancelot & P. Wassmann) *Journal of Marine Systems* **5**, 5-22.
760
761 Simon, N., Campbell, L., Örnolfsdottir, E., Groben, R., Guillou, L., Lange, M.,
762 Medlin, L.K. (2000) Oligonucleotide probes for the identification of three algal
763 groups by dot blot and fluorescent whole-cell hybridization. *J. Eukaryot.*
764 *Microbiol*. **47**, 76-84.
765
766 Sun, Q., Chu, G., Liu, G., Li S., and Wang X. (2007) Calibration of alkenone
767 unsaturation index with growth temperature for a lacustrine species,
768 Chrysotila lamellose (Haptophytceae). *Organic Geochemistry* **38**, 1226-1234.
769

770 Theroux, S., D'Andrea, W.J., Toney, J.L., Amaral-Zettler, L., Huang, Y.
771 (2010) Phylogenetic diversity and evolutionary relatedness of alkenone-
772 producing haptophyte algae in lakes: Implications for continental
773 paleotemperature reconstructions. *Earth and Planetary Science Letters* **300**,
774 311-320.
775
776 Thiel V., Jenisch A., Landmann G., Reimer A., and Michaels W. (1997)
777 Unusual distributions of long-chain alkenones and tetrahymanol from the
778 highly alkaline Lake Van, Turkey. *Geochimica et Cosmochimica Acta* **61**,
779 2053-2064.
780
781 Toney, J.L., Huang, Y., Fritz, S.C., Baker, P.A., Grimm, E., and Nyren, P.
782 (2010) Climatic and environmental controls on the occurrence and
783 distribution of long chain alkenones in lakes. *Geochimica et Cosmochimica*
784 *Acta* **74**, 1563-1578.
785
786 Volkman J.K., Eglinton G., Corner E.D.S., and Forsberg T.E.V. (1980) Long-
787 chain alkenes and alkenones in the marine coccolithophorid *Emiliania*
788 *huxleyi*. *Phytochemistry* **19**, 2619-2622.
789

790 Volkman J.K., Burton H.R., Everitt D.A., and Allen D.I. (1988) Pigment and
791 lipid composition of algal and bacterial communities in Ace Lake, Vestfold
792 Hills, Antarctica. *Hydrobiologia* **165**, 41-57.
793
794 Volkman, J.K., Barrett, S.M., Blackburn, S.I., Sikes, E.L. (1995) Alkenones in
795 *Gephyrocapsa oceanica*: Implications for studies of paleoclimate. *Geochim.*
796 *Cosmo. Acta* **3**, 513-520.
797
798 Wang R. and Zheng M. (1998) Occurrence and environmental significance of
799 long-chain alkenones in Tibetan Zabuye Salt Lake, SW China. *Int. J. Salt*
800 *Lake Res.* **6**, 281–302.
801
802 Zink K.G., Leythaeuser D., Melkonian, M., and Schwark, L. (2001)
803 Temperature dependency of long-chain alkenone distributions in recent to
804 fossil limnic sediments and in lake waters. *Geochimica et Cosmochimica Acta*
805 **65**, 253-265.
806

FIGURE CAPTIONS

Figure 1. GC-FID traces for alkenone-containing enrichments A-E (lower) and surface sediment (upper).

Figure 2. A consensus Bayesian phylogenetic tree showing the 18S rRNA gene-inferred relationships among haptophyte algae in the GenBank database. Sequences reported in this study, Hap-A and Hap-B, are in bold. Details on numbered OTUs and Greenland group are reported by Theroux et al., (2010). Numbers above branch points represent posterior probability values.

Figure 3. (left panel) Shows the temperature dependence of the □ and □ indices in week 6 and week 2, respectively for Hap-A enrichments. This is offset from the *in situ* calibration from Lake George (circles) reported be Toney et al., (2010). (right panel) Shows the reduction in percent $C_{37:4}$ at all temperatures for Hap-A enrichments.

Figure 4. FISH using haptophyte-specific probes. (a) Light microscope image of Hap-A, and (b) the same cell showing probe fluorescence. (c) Hap-B under phase microscopy and (d) green fluorescence from haptophyte probe with red chloroplasts due to natural autofluorescence.

Figure 1.

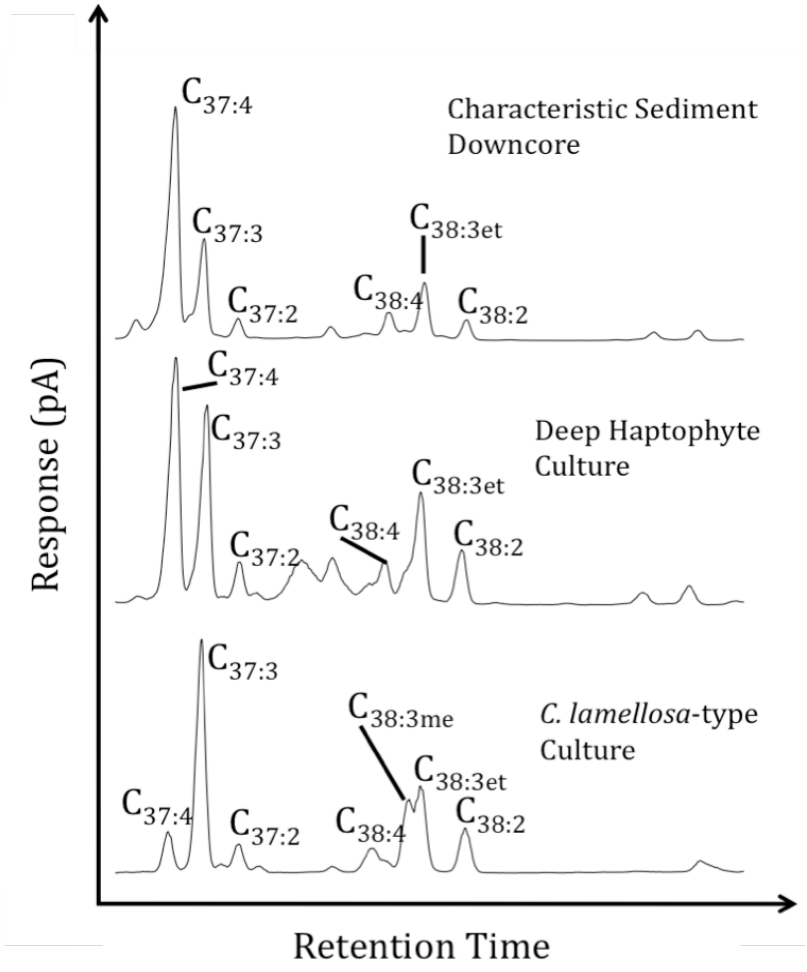
Response (pA)
Retention Time
C37:4
C37:3
C37:2
C38:4
C38:3et
C38:2
Characteristic Sediment Downcore
Deep Haptophyte Culture
C38:3me
C. lamellosa-type Culture

Figure 2.

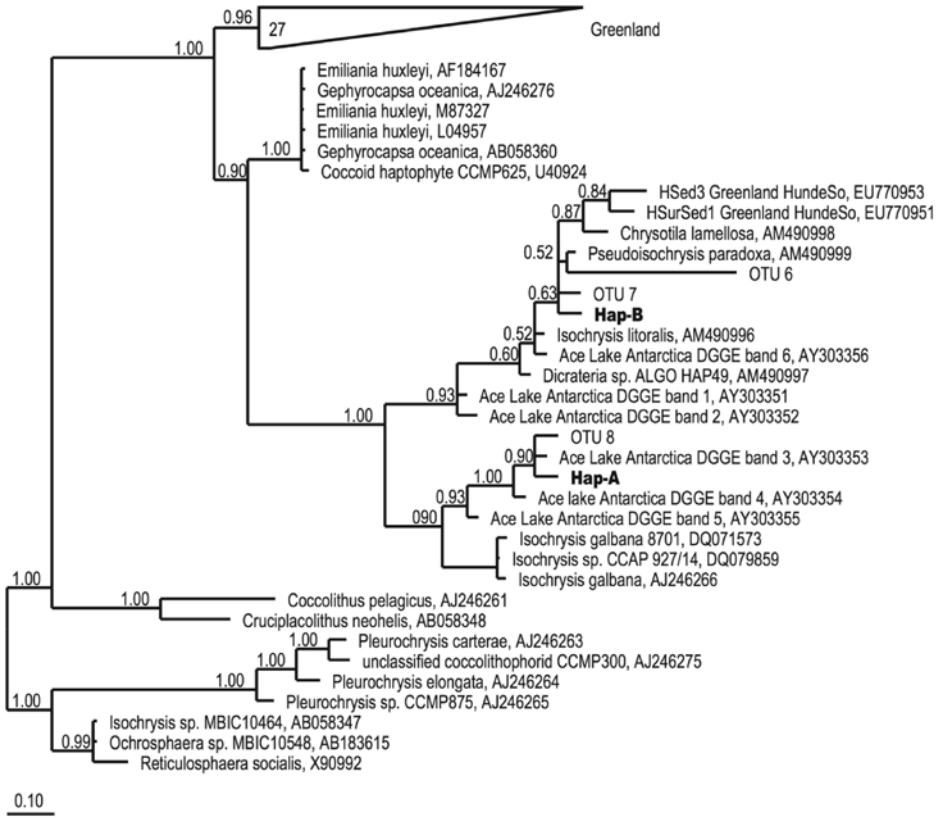
0.96
27
Greenland
1.00
Emiliania huxleyi, AF184167
Gephyrocapsa oceanica, AJ246276
Emiliania huxleyi, M87327
Emiliania huxleyi, L04957
1.00
Gephyrocapsa oceanica, AB058360
0.90
Coccoid haptophyte CCMP625, U40924
0.84
HSed3 Greenland HundeSo, EU770953
0.87
HSurSed1 Greenland HundeSo, EU770951
Chrysotila lamellosa, AM490998
0.52
Pseudoisochrysis paradoxa, AM490999
OTU 6
0.63
OTU 7
Hap-B
0.52
Isochrysis litoralis, AM490996
0.60
Ace Lake Antarctica DGGE band 6, AY303356
Dicrateria sp. ALGO HAP49, AM490997
0.93
Ace Lake Antarctica DGGE band 1, AY303351
1.00
Ace Lake Antarctica DGGE band 2, AY303352
OTU 8
0.90
Ace Lake Antarctica DGGE band 3, AY303353
1.00
Hap-A
0.93
Ace lake Antarctica DGGE band 4, AY303354
090
Ace Lake Antarctica DGGE band 5, AY303355
Isochrysis galbana 8701, DQ071573
Isochrysis sp. CCAP 927/14, DQ079859
Isochrysis galbana, AJ246266
1.00
1.00
Coccolithus pelagicus, AJ246261
Cruciplacolithus neohelis, AB058348
1.00
Pleurochrysis carterae, AJ246263
1.00
unclassified coccolithophorid CCMP300, AJ246275
1.00
Pleurochrysis elongata, AJ246264
1.00
Pleurochrysis sp. CCMP875, AJ246265
Isochrysis sp. MBIC10464, AB058347
0.99
Ochrosphaera sp. MBIC10548, AB183615
Reticulosphaera socialis, X90992
0.10

Figure 3.

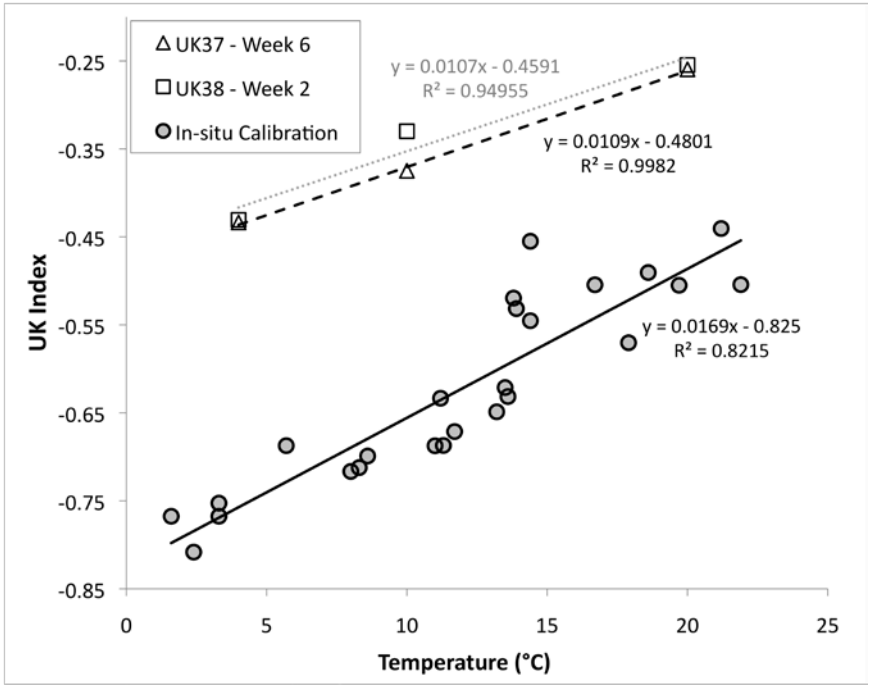
UK37 - Week 6
UK38 - Week 2
In-situ Calibration
y = 0.0107x - 0.4591
R² = 0.94955
y = 0.0109x - 0.4801
R² = 0.9982
y = 0.0169x - 0.825
R² = 0.8215
UK Index
Temperature (°C)
-0.25
-0.35
-0.45
-0.55
-0.65
-0.75
-0.85
0
5
10
15
20
25

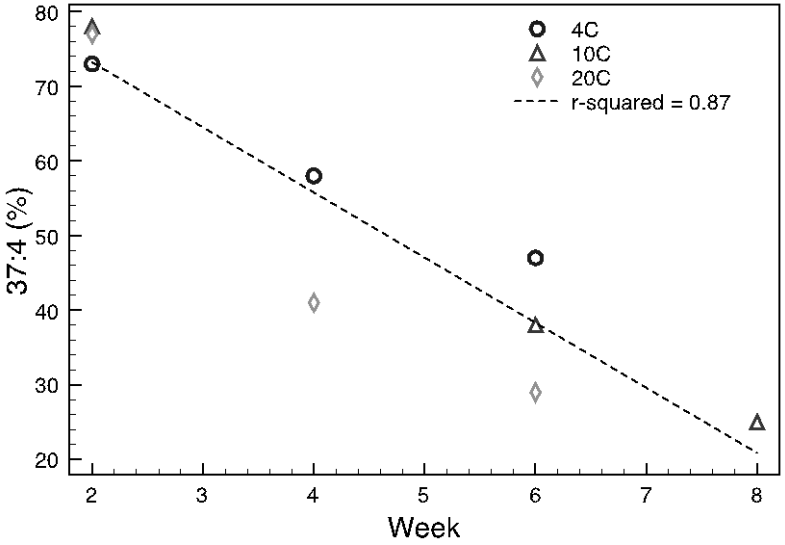
4C
10C
20C
r-squared = 0.87
37:4 (%)
Week
80
70
60
50
40
30
20
2
3
4
5
6
7
8

Figure 4.

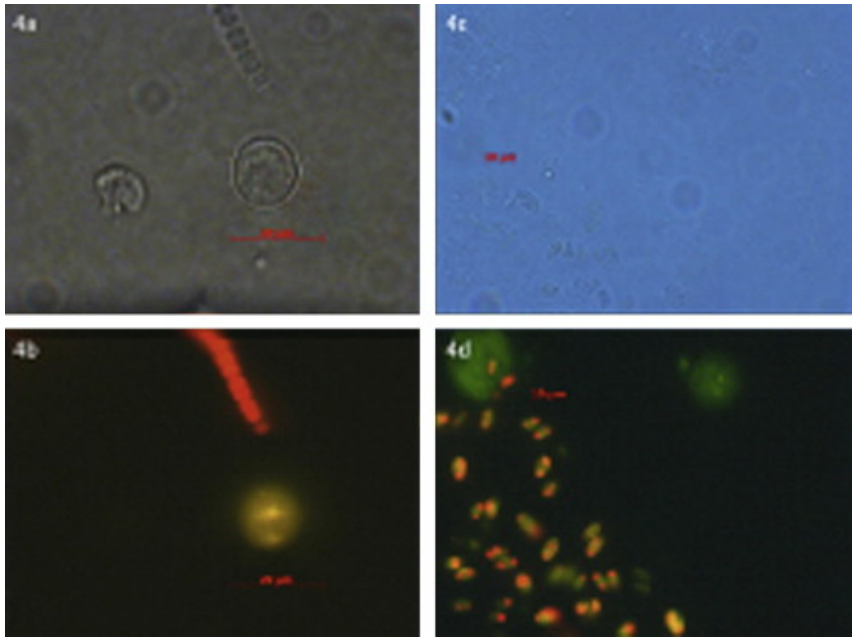

Table 1.

ID	Start date	Enrichment origin	GPS Collection Location	Culture medium	Observations (April 2010)	LCAs April 2010	C37:4	C37:3	C37:2	[37] (ug/L)	37:38	UK37	UK'37	UK38	UK37 Inferred T (°C)	*C. lamellosa* calib.
A	6/9/09	10-m depth water column	N46°44.375, W099°29.622	filtered lake water, f/2 nutrient medium	distinct dark green, globular colonies floating, brownish coccoid cells that might be haptophytes; a Nannochloropsis-like greenish coccoid; a flagellate that looks like Ochromonas triangulata	Y	2.103	7.922	0.832	10.42	1.18	-0.12	0.10	0.32	36.47	12.79
B	6/9/09	5-m depth water column	N46°45.014, W099°29.468	filtered lake water, f/2 nutrient medium	red cyanobacterial mat on bottom of culture flask, lots of brownish coccoid cells	Y	22.375	132.460	14.656	153.27	1.14	-0.05	0.10	0.13	39.94	14.69
C	6/9/09	near shore sediment (4.5-m depth)	N46°45.045, W099°29.442	filtered lake water, f/2 nutrient medium	brown bubbly foam at surface, greenish/gray fatty material below, Chromulina-like cells; Oedogonium filaments; Hateria (a ciliate); Chroococcus and other Cyanobacteria; Arcellus; a tenticle-bearing pedinellid; a very few coccoid brownish cells	Y	26.537	132.688	16.511	140.65	1.40	-0.06	0.11	0.19	39.38	14.38
D	6/9/09	6-m depth water column	N46°44.375, W099°29.622	filtered lake water, f/2 nutrient medium	red bacterial mat on bottom of culture flask, Chromulina-like cells; Pavlova-like cells; Brownish cell in gel that looks like it may be a Haptophyte; a flagellate; and the brown mat is a cyanobacterial mat	Y	16.787	83.048	7.067	122.02	1.26	-0.09	0.08	0.16	37.74	13.48
E	6/9/09	deep sediment (44-m depth)	N46°44.342, W099°29.376	filtered lake water, *f*/2 nutrient medium	similar to B, but brown/green mat of bubbles suspended mid-flask, Lots of cyanobacterial filaments; lots of brown coccoid cells that might be haptophytes; some cells that look like dormant green algae; a loricate cell of Paulinella	Y	892.656	674.458	96.063	1191.59	1.80	-0.48	0.12	0.20	18.92	3.19
F	6/9/09	10-m depth water column	N46°44.375, W099°29.622	diluted sea water, *f*/2 nutrient medium	thin orange mats, a couple of dead diatoms and a living filament of a cyanobacterium	N	x	x	x	x	x	x	x	x	x	x

Growth Chamber Conditions (07/12/09 to 02/15/10):20°C light, 18°C dark, 68% humidity, 12hr light: 12hr dark

Table 2.

Ion	Seawater[a]	Lake George[a]	SW_{NORM}	LG_{NORM}	LG relative to SW
Mg^{2+}	1300	400	0.06	0.05	0.31
Na^{+}	11000	3056	0.58	0.41	0.28
Ca^{2+}	400	11.8	0.01	0.00	0.03
K^{+}	380	250	0.01	0.03	0.66
Cl^{-}	19000	724	1.00	0.10	0.04
$SO4^{2-}$	2600	7370	0.13	1.00	2.83
$CO3^{2-}/HCO3^{-}$	142	346	0.00	0.05	2.44

[a]Units are in mg L^{-1}

Table 3.

Collection Date (m/dd)	Enrichment ID	Growth Chamber Temp (°C)	LCA Presence	C37:4	C37:3	C37:2	Sum 37	C38:4	C38:3	C38:2	sum 38	[C37] (ug L^{-1} water)	UK'37	UK37	UK38	UK38'	UK3738	C37/C38	%37:4	Inferred Temp. (°C)
7/13	CONTROL	4	N	x	x	x	x	x	x	x	x	x	x	x	x	x	x	x	x	x
7/13	CONTROL	10	N	x	x	x	x	x	x	x	x	x	x	x	x	x	x	x	x	x
7/13	CONTROL	20	N	x	x	x	x	x	x	x	x	x	x	x	x	x	x	x	x	x
7/27	CONTROL	4	Y	4.13	9.83	0.72	14.68	3.64	13.86	2.51	20.01	18.92	0.068	-0.23	-0.06	0.15	0.12	0.73	28	31
7/27	CONTROL	10	Y	50.44	68.63	13.32	132.38	33.07	35.77	3.92	72.77	164.44	0.162	-0.28	-0.40	0.10	0.14	1.82	38	29
7/27	CONTROL	20	N	x	x	x	x	x	x	x	x	x	x	x	x	x	x	x	x	x
8/10	CONTROL	4	Y	36.36	134.13	1.12	171.61	145.13	643.16	156.24	944.53	179.29	0.008	-0.21	0.01	0.20	0.17	0.18	21	32
8/10	CONTROL	10	Y	43.25	99.95	4.83	148.04	107.11	274.49	44.79	426.39	122.19	0.046	-0.26	-0.15	0.14	0.12	0.35	29	30
8/10	CONTROL	20	N	x	x	x	x	x	x	x	x	x	x	x	x	x	x	x	x	x
8/25	CONTROL	4	Y	1.41	5.34	0.001	6.75	18.24	22.67	5.96	46.86	49.17	0.00019	-0.21	-0.26	0.21	0.18	0.14	21	32
8/25	CONTROL	10	N	x	x	x	x	x	x	x	x	x	x	x	x	x	x	x	x	x
8/25	CONTROL	20	N	x	x	x	x	x	x	x	x	x	x	x	x	x	x	x	x	x
7/13	DEEP	4	Y	48.85	15.98	1.74	66.57	9.56	7.11	1.66	18.33	49.66	0.098	-0.71	-0.43	0.19	0.13	3.63	73	8
7/13	DEEP	10	Y	19.48	4.97	0.44	24.89	4.36	3.83	1.25	9.44	20.34	0.080	-0.77	-0.33	0.25	0.16	2.64	78	5
7/13	DEEP	20	Y	16.23	3.91	1.06	21.20	2.90	3.19	1.08	7.17	18.42	0.213	-0.72	-0.25	0.25	0.23	2.96	77	7
7/27	DEEP	4	Y	48.42	34.66	0.01	83.09	45.79	164.31	45.47	255.57	55.77	0.0003	-0.58	0.00	0.22	0.19	0.33	58	14
7/27	DEEP	10	Y	6.41	9.25	0.11	15.77	8.57	21.58	3.04	33.19	20.37	0.012	-0.40	-0.17	0.12	0.09	0.47	41	23
7/27	DEEP	20	N	x	x	x	x	x	x	x	x	x	x	x	x	x	x	x	x	x
8/10	DEEP	4	Y	68.79	72.99	5.10	146.88	73.14	250.70	69.78	393.62	204.61	0.065	-0.43	-0.01	0.22	0.19	0.37	47	21
8/10	DEEP	10	Y	322.80	510.68	7.52	841.00	825.67	2347.00	515.53	3688.20	418.40	0.015	-0.37	-0.08	0.18	0.15	0.23	38	24
8/10	DEEP	20	Y	43.25	99.95	4.83	148.04	107.11	811.40	2364.76	529.09	122.19	0.046	-0.26	0.69	0.74	0.72	0.28	29	30
8/25	DEEP	4	N	x	x	x	x	x	x	x	x	x	x	x	x	x	x	x	x	x
8/25	DEEP	10	Y	0.36	1.06	0.001	1.42	1.71	4.47	1.44	7.63	34.59	0.745	-0.25	-0.04	0.24	0.34	0.19	25	30
8/25	DEEP	20	N	x	x	x	x	x	x	x	x	x	x	x	x	x	x	x	x	x
8/25	DEEP TURB	4	Y	103.78	253.17	2.74	131.70	18.24	22.67	5.96	46.86	601.06	0.098	-0.28	0.02	0.21	0.15	2.81	79	5
8/25	DEEP TURB	10	Y	159.90	231.27	16.38	407.55	349.86	1066.00	265.70	1681.56	697.35	0.066	-0.35	-0.05	0.20	0.18	0.24	39	25
8/25	DEEP TURB	20	N	x	x	x	x	x	x	x	x	x	x	x	x	x	x	x	x	x
7/13	UNFILT	4.0	N	x	x	x	x	x	x	x	x	x	x	x	x	x	x	x	x	x
7/13	UNFILT	10	N	x	x	x	x	x	x	x	x	x	x	x	x	x	x	x	x	x
7/13	UNFILT	20	N	x	x	x	x	x	x	x	x	x	x	x	x	x	x	x	x	x
7/27	UNFILT	4	Y	8.89	26.79	0.01	35.69	23.66	102.42	11.75	137.83	24.85	0.00037	-0.25	-0.09	0.10	0.08	0.26	25	30
7/27	UNFILT	10	Y	49.83	68.75	10.64	129.21	29.06	20.04	3.93	53.03	117.81	0.134	-0.30	-0.47	0.16	0.14	2.44	39	27
7/27	UNFILT	20	N	x	x	x	x	x	x	x	x	x	x	x	x	x	x	x	x	x
8/10	UNFILT	4	N	x	x	x	x	x	x	x	x	x	x	x	x	x	x	x	x	x
8/10	UNFILT	10	Y	19.58	52.49	0.82	72.89	69.47	234.37	48.16	351.99	76.82	0.015	-0.26	-0.06	0.17	0.15	x	27	30
8/10	UNFILT	20	N	x	x	x	x	x	x	x	x	x	x	x	x	x	x	x	x	x
8/25	UNFILT	4	N	x	x	x	x	x	x	x	x	x	x	x	x	x	x	x	x	x
8/25	UNFILT	10	Y	0.72	1.90	0.001	2.62	1.97	5.64	1.47	9.08	19.21	0.001	-0.274	-0.054	0.207	0.164	0.289	27	29
8/25	UNFILT	20	N	x	x	x	x	x	x	x	x	x	x	x	x	x	x	x	x	x

Table 4.

Lake	Location	Latitude	Longitude	Depth (m)	pH	Salinity (g L^{-1})	Na	K	Mg	Ca	CO_3	HCO_3	Cl	SO_4	Source
Lake George	North Dakota, USA	46.74	-99.49	60	9	9.7	3056	250	400	11.83	346.4	nd	1292	12210	Toney et al. 2010
Medicine Lake	South Dakoata, USA	44.82	-97.37	8.3	8.4	9	nd	nd	nd	nd	245	nd	605	28680	Toney et al. 2010
Skoal Lake	North Dakota, USA	47.92	-101.47	1.8	8.9	8	nd	nd	nd	nd	276.9	nd	155.2	8955	Toney et al. 2010
Pyramid Lake	Nevada, USA	40	-119.5	59	9.3	5	1720	118	114	9.3	300	860	2080	280	Galat et al. 1981
Tso Ur	Tibetan Plateau, China	31.48	91.52	8.4	9.8	12	3467.9	249.7	110.7	7.9	638	4240	1234.1	1967.8	Wu et al. 2009

nd = not determined

Anion and cation units are mg L^{-1}